Cooperative planning model of renewable energy sources and energy storage units in active distribution systems

A bi-level model and Pareto analysis

Li, Rui; Wang, Wei; Wu, Xuezhi; Tang, Fen; Chen, Zhe

Published in:
Energy

DOI (link to publication from Publisher):
10.1016/j.energy.2018.11.069

Publication date:
2019

Document Version
Accepted author manuscript, peer reviewed version

Accepted Manuscript

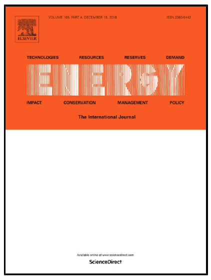

Cooperative Planning Model of Renewable Energy Sources and Energy Storage Units in Active Distribution Systems: A Bi-level Model and Pareto Analysis

Rui Li, Wei Wang, Xuezhi Wu, Fen Tang, Zhe Chen

PII:	S0360-5442(18)32281-3
DOI:	10.1016/j.energy.2018.11.069
Reference:	EGY 14167
To appear in:	*Energy*
Received Date:	10 April 2018
Accepted Date:	17 November 2018

Please cite this article as: Rui Li, Wei Wang, Xuezhi Wu, Fen Tang, Zhe Chen, Cooperative Planning Model of Renewable Energy Sources and Energy Storage Units in Active Distribution Systems: A Bi-level Model and Pareto Analysis, *Energy* (2018), doi: 10.1016/j.energy.2018.11.069

Cooperative Planning Model of Renewable Energy Sources and Energy Storage Units in Active Distribution Systems: A Bi-level Model and Pareto Analysis

Rui LI[1], Wei WANG[1], Xuezhi WU[1], Fen TANG[1], Zhe CHEN[2]

1. National Active Distribution Network Technology Research Center, Beijing Jiaotong University, Beijing 100044, China

2. Department of Energy Technology, Aalborg University, Aalborg DK9220, Denmark

Correspondence information: Rui LI

Affiliation: National Active Distribution Network Technology Research Center, Beijing Jiaotong University.

Address: Rm. 510, Building of Electrical Engineering, Beijing Jiaotong University, No3. ShangYuanCun, Haidian District, Beijing, China.

Email address: lirui_ee @bjtu.edu.cn

Telephone number: +86 156-2496-0215

Cooperative Planning Model of Renewable Energy Sources and Energy Storage Units in Active Distribution Systems: A Bi-level Model and Pareto Analysis

A. Rui LI [a*], B. Wei WANG[a], C. Xuezhi WU[a], D. Fen TANG[a], E. Zhe CHEN[b]

[a] National Active Distribution Network Technology Research Center,
Beijing Jiaotong University, Beijing 100044, China
[b.] Department of Energy Technology, Aalborg University, Aalborg DK9220, Denmark

ABSTRACT

This paper proposes a multi-objective, bi-level optimization problem for cooperative planning between renewable energy sources and energy storage units in active distribution systems. The multi-objective upper level serves as the planning issues to determine the sizes, sites, and types of renewable energy sources and energy storage units. The fuzzy multi-objective lower level serves as the operation issues to formulate operation strategy and determine the schedules of energy storage units. By means of bi-level programming, the optimal operation strategy of energy storage units is incorporated into the upper level and optimized with planning issues cooperatively. Meanwhile, to address high-level uncertainties and simultaneously capture the temporal correlation related to renewable energy sources, electric vehicles, and load demands, the validity index of Davies Bouldin is adopted to develop sets of probabilistic scenarios with high quality and diversity. A hierarchical solving strategy based on modified particle swarm optimization is applied to solve the bi-level nonlinear, mixed integer optimization problem. Results and further analyses demonstrate that the proposed planning model and optimization methods have the ability to allocate renewable energy sources and energy storage units effectively for reducing costs, enhancing reliability, and promoting clean energy.

Keywords: Active distribution system, renewable energy source, energy storage, bi-level programming, Pareto analysis, planning

* Rui LI. Tel.: +86 156-2496-0215; fax: +86 5168 4873. E-mail address: lirui_ee@bjtu.edu.cn

Nomenclature

A. Abbreviations

ADS	Active distribution system
DER	Distributed energy resource
DG	Distributed generation
EENS	Expected energy not supplied
ESU	Energy storage unit
EV	Electric vehicle
O&M	Operation and maintenance
OPF	Optimal power flow
MOPSO	Multi-objective particle swarm optimization algorithm
MODE	Multi-objective differential evolution algorithm
PV	Photovoltaic
PSO	Particle swarm optimization algorithm
RES	Renewable energy source
RESP	RES penetration
SOC	State of charge
TOU	Time of use
WG	Wind generator

B. Sets

$\Omega_{\mathrm{WG}}, \Omega_{\mathrm{PV}}, \Omega_{\mathrm{ESU}}, \Omega_{\mathrm{bus}}, \Omega_{\mathrm{line}}$	Sets of WG/PV/ESU/load bus/line

C. Variables

$P_m^{\mathrm{PV,rated}}, P_n^{\mathrm{WG,rated}}$	Power rating of PV *m*/WG *n*
$v_{\mathrm{ci}}, v_{\mathrm{co}}, v_{\mathrm{rated}}$	Cut-in/cut-out/rated wind speed for WG
v_t	Wind speed at time *t*
a, *b*	Parameters of power characteristic model of WG
$\varepsilon^{\mathrm{PV}}$	Module conversion efficiency of PV
e_t	Solar irradiance at time *t*
S_m^{PV}	Total area of PV *m*
$P_{i,t}^{\mathrm{RL}}, P_{i,t}^{\mathrm{EV}}$	Regular load/EVs charging load of bus *i* at time *t*
$P_i^{\max}$	Maximum of regular load demands at time *t*
R_w	Weekly peak load in percent of annual peak load
R_d	Daily peak load in percent of weekly peak load
R_h	Hourly peak load in percent of daily peak load
$\Delta P_t^{\mathrm{load}}$	Random fluctuation of regular load at time *t*
$t^{\mathrm{arr}}, t^{\mathrm{dep}}$	Arrival time/departure time of EV
$\mu^{\mathrm{arr}}, \sigma^{\mathrm{arr}}$	Mean value/standard deviation with respect to arrival time
$\mu^{\mathrm{dep}}, \sigma^{\mathrm{dep}}$	Mean value/standard deviation with respect to departure time
d^{dri}	Driving distance of EV
$\mu^{\mathrm{dri}}, \sigma^{\mathrm{dri}}$	Mean value/standard deviation with respect to driving distance
E_f^{demand}	Daily electricity demand of EV *f*
$W_f^{\mathrm{EV,rated}}$	Unit energy consumption rating of EV *f*
$P_f^{\mathrm{EV,rated}}$	Charging power rating of EV *f*
$P_{f,t}^{\mathrm{EV}}$	Charging power of EV *f* at time *t*
$E_{f,t}^{\mathrm{EV}}$	Energy stored in battery bank of EV *f* at time *t*
η_f^{C}	Charging efficiency of EV *f*
I^{DB}	Cluster validity index of Davies Bouldin
N^{SC}	Number of cluster center for k-means clustering
N_g	Number of vectors in cluster center *g*
S_h	Dispersions of cluster center *h*

d_{gh}	Distance between cluster center g and cluster center h
C_h	Cluster center h
$C_{\mathrm{d}}^{\mathrm{inv}}, C_{\mathrm{d}}^{\mathrm{mai}}, C_{\mathrm{d}}^{\mathrm{ope}}$	Diurnal investment/maintenance/operation cost
$cc^{\mathrm{PV}}, cc^{\mathrm{WG}}$	Unit capital cost of PV/WG
$cc_k^{\mathrm{PCS}}, cc_k^{\mathrm{B\&R}}$	Unit capital cost of ESU k related to power conversion system/storage banks
$\delta^{\mathrm{PV}}, \delta^{\mathrm{WG}}, \delta_k^{\mathrm{ESS}}$	Capital recovery factor of PV/WG/ESU k
$P_k^{\mathrm{ESS,rated}}, S_k^{\mathrm{ESS,rated}}$	Power rating/energy capacity of ESU k
$cm^{\mathrm{PV}}, cm^{\mathrm{WG}}$	Unit O&M cost of PV/WG
$cm_k^{\mathrm{FOM}}, cm_k^{\mathrm{VOM}}$	Unit fixed/variable O&M cost of ESU k
ω_{sc}	Probability of scenario sc occurrence
$h_{k,sc}$	Operation hours of ESU k in scenario sc
CO_{sc}^{net}	Diurnal operation cost of network in scenario sc
EP_t	TOU electricity price at time t
$P_{m,sc,t}^{\mathrm{PV}}, Q_{m,sc,t}^{\mathrm{PV}}$	Active/reactive power output of PV m at time t in scenario sc
$P_{n,sc,t}^{\mathrm{WG}}, Q_{n,sc,t}^{\mathrm{WG}}$	Active/reactive power output of WG n at time t in scenario sc
$P_{sc,t}^{\mathrm{TL}}, Q_{sc,t}^{\mathrm{TL}}$	Total active/reactive load demands at time t in scenario sc
$P_{i,sc,t}^{\mathrm{RL}}, Q_{i,sc,t}^{\mathrm{RL}}$	Regular load demands of bus i at time t in scenario sc
$P_{i,sc,t}^{\mathrm{EV}}$	EVs charging load demands of bus i at time t in scenario sc
$P_{l,sc,t}^{\mathrm{loss}}$	Active losses of line l at time t in scenario sc
$P_{k,sc,t}^{\mathrm{ESU}}$	Active power absorption/output of ESU k at time t in scenario sc
$T^{\mathrm{PV}}, T^{\mathrm{WG}}, T_k^{\mathrm{ESU}}$	Product lifetime of PV/WG/ESU k
r	Rate of interest
$I_{l,sc,t}$	Electric current for line l at time t in scenario sc
R_l	Resistance of line l
I_{sc}^{EENS}	Mean value of EENS for scenario sc
$I_{sy,sc}^{\mathrm{EENS}}$	EENS for scenarios sc in statistic year sy
N^{sy}	Number of statistic year
$Pen_{\mathrm{d}}^{\mathrm{RES}}$	Diurnal average RES penetration
Pen_{sc}^{RES}	RES penetration in scenario sc
W_{sc}^{RES}	Energy supplied by RESs in scenario sc
W_{sc}^{TL}	Energy of total load demands in scenario sc
$\pi_{k,sc}^{\mathrm{ESU}}$	Diurnal benefit of ESU k in scenario sc
$P_{k,sc,t}^{\mathrm{ESU,ava}}$	Reserve capability of ESU k at time in scenario sc
$SOC_{k,sc,t}$	SOC for ESU k at time t in scenario sc
$SOC_k^{\max}, SOC_k^{\min}$	Permissible range of SOC for ESU k
$\eta_k^{\mathrm{C}}, \eta_k^{\mathrm{D}}$	Charging/discharging efficiency of ESU k
μ^{L}	Fuzzy satisfactory degree of multi-objective of lower level
$\mu\left(F_1^{\mathrm{L}}\right), \mu\left(F_2^{\mathrm{L}}\right)$	Fuzzy membership degree of objectives of lower level
λ^{I}	Maximum proportion of RES installation capacity
S^{sub}	Power rating of HV/MV substation
$P_{sc,t}^{\mathrm{sub}}, Q_{sc,t}^{\mathrm{sub}}$	Active/reactive power output of HV/MV substation at time t in scenario sc
$P_{i,sc,t}, Q_{i,sc,t}$	Net active/reactive power of bus i at time t in scenario sc
$U_{i,sc,t}$	Voltage magnitude of bus i at time t in scenario sc

$\theta_{ij,sc,t}$	Voltage angle difference between bus *i* and bus *j* at time *t* in scenario *sc*
G_{ij}, B_{ij}	Transfer conductance and susceptance between bus *i* and bus *j*
$U_i^{\max}, U_i^{\min}$	Permissible range of voltage magnitude for bus *i*
$I_l^{\max}$	Maximum of electric current for line *l*
$E_{k,sc,t}^{\mathrm{ESU}}$	Energy stored in the battery bank of ESU *k* at time *t* in scenario *sc*
MTTF, MTTR	Mean time to failure/ mean time to repair

D. Index

i, *j*	Bus
L	line
M	PV
N	WG
K	ESU
F	EV
T	Hour
W	Week
D	Day
Sc	Scenario
Sy	Statistic year
g,h	Cluster center
u,v	Iterations of upper level/lower level

1. INTRODUCTION

The proliferation of distributed energy resources (DERs), particularly wind generators (WGs), photovoltaics (PVs), and energy storage units (ESUs), together with flexible load growth has significantly changed planning methods of distribution systems. The aim of this paper is to introduce a cooperative planning model of active distribution systems (ADSs) to determine sizes, sites, and types of RESs and ESUs properly.

1.1 Motivation

Given the challenges related to the dependency from fossil fuels and environmental degradation, DERs, particularly variable renewable energy sources (RESs) experience a rapid expansion all over the world, and a more accelerated growth is expected by 2020 [1]. Therefore, energy systems, particularly power systems, have been in transition towards increased flexibility in operation, which will bring potential economic benefits [2]. Studies have shown that the proliferation of DERs is expected to be the available solution to deal with power demand growth and provide a practicable approach to achieve sustainable energy development. For instance, Bornholm Island in Denmark [3] and Kitami City in Japan [4] are seeking ways to achieve a 100% renewable energy system. Despite their advantages, RESs are characterized by considerable instability and intermittent nature [5], which pose a number of challenges to distribution systems [6]. Furthermore, the widespread use of electric vehicles (EVs) aggravates these challenges.

In recent years, the deterministic strategy called "fit and forget" are widely adopted to deal with the integration of variable DERs, which in some extent ignores these undesirable influences and potential benefits. Therefore, the flexibility potential from these widely-used DERs requires a change in the present paradigm [7]. To address this problem, ADS is introduced to manage these DERs in an economical and efficient way, and to make them take some degree of responsibility for system supply [8]. Obviously, DERs play a more and more important role in ADSs and have become the key elements to assist distribution system operators in an optimal manner [9]. Therefore, how to determine the proper sizes, sites, and types of DERs has attracted widespread attention of researchers.

1.2 Literature review

In [10], a planning method for distributed generations (DGs) in ADSs is introduced, where active power curtailment, voltage control, and reactive power compensation are coupled to alleviate the impacts on RESs accommodation brought by voltage constraints. Different from [10], in [11], the cooperative reactive power control of multi-WG is adopted in the proposed model based on multi-period optimal power flow (OPF) to exploit the maximum wind energy capacity. The authors in [12] analyze the influences of various multi-DG configurations and propose a planning model to determinate the capacities and locations for multiple WGs based on the multi-configuration, multi-period OPF. In [13], to reduce energy losses, a combination of DGs and RESs is allocated optimally. To capture the time-varying characteristics, just four seasonal typical scenarios are adopted to represent variation of power generations and load demands. Tanwar and Khatod [14] adopt analytic hierarchy process and particle swarm optimization (PSO) to solve a proposed multi-objective planning model to determine sizes and sites of dispatchable DGs and non-dispatchable DGs. In this article, five performance indices are taken into consideration including power loss, maximum branch current capacity, voltage deviation, economics and environment impact. Literature on DGs planning is rich, but few of these works consider allocating RESs and ESUs cooperatively.

ESUs have the flexible ability to regulate active power and energy, and thereby the optimal allocation of ESUs is beneficial for ADSs. From this perspective, these articles, which follow, are especially important. To accommodate wind energy, a multi-step ESUs planning mode is presented in [15] to minimize the annual costs. This is a prior paper adopting ESUs to increase the hosting capacity for wind energy. Authors in [16] take advantage of optimal allocation of ESUs to shave peak load demands, regulate voltage, and improve reliability of system, where all these three roles are formulated as monetary items and penalty factors, respectively. In [17], for the purpose of maximizing the size of renewable power absorbed by distribution networks, a mixed integer linear programming optimization is proposed to determine the sizes, sites, and time of DGs and ESUs simultaneously. Research [18] formulates the optimal planning of ESUs as a nonlinear, mixed integer optimization problem to maximize the profit of distribution company, where optimal active power and reactive power are denoted for ESUs and DGs simultaneously. In order to tackle the uncertainties related to wind-solar units and relief congestion in the electric power lines, an optimal model for planning and scheduling on ESUs is presented in [19]. For further reading, a recent feature paper [20] is recommended on the issue of combined resources allocation, where a combined model formulation is introduced to allocate the EVs charging stations, RESs and ESUs in distribution networks. To enhance the accuracy of the resource allocation problem, the cooperative control of EVs charging, RESs output power, and ESUs charging/discharging are incorporated in the formulated model. Additionally, to maximize investment benefits and to minimize power losses, the planning problem of DGs and ESUs is programmed as a two-stage optimization model in [21], where the first stage is adopted to determine the sites and sizes of DGs and the second stage serves to identify optimal installation capacities of DGs. In the optimizing process, maximum outputs of ESUs are determined to address the uncertain outputs of DGs based on chance-constrained programming.

From the above brief survey, it can be observed that although many attempts have been made, some problems of cooperative planning between RESs and ESUs have not been tackled yet. Firstly, most planning models pay little attention to the refined simulation of ESUs operation; the appropriate operation strategy is not taken into account adequately in most planning models. The simple models without optimization in existing works have little ability to represent the time-dependence operation schedules and diverse important roles of ESUs in the planning process, such as promoting economic efficiency, enhancing reliability, improving power quality and RESs penetration (RESP).

Secondly, the frequently used probabilistic models such as Beta distribution [22], Weibull distribution [23], Gaussian distribution [19] and Normal distribution [24] cannot effectively capture the time-variable nature and the inherent simultaneity between multiple RESs and load demands. Thus, the temporal complementarity of multiple RESs, and temporal correlation between power outputs and load demands may escape from researchers' notice. More importantly, the operation schedules of ESUs based on these profiles without timing consideration may be incorrect because of the strict timing sequence constraints of ESUs.

Thirdly, economic issues are always adopted to be planning objectives without adequate considerations about reliability and eco-friendly issues. Even if some of them have considered these factors, they always convert them into economic items, such as outage cost and emission tax. Hence, the values of these economic items influence the quality and optimality of obtained solutions. In other words, these approaches with a priori articulation of preferences have the drawback of subjectivity. Therefore, these studies without multiple criteria decision analysis can not select targeted planning schemes from different perspectives, which is no longer valid for the flexible ADSs planning [25].

1.3 Contributions

To address these three major issues, the aim of this paper is to introduce a cooperative planning model and optimization methods to find cost-effective, reliable and environmentally friend planning solutions. Meanwhile, the emphasis is also given on the collaborative optimization between planning issues and operation issues in different time scales. Compared to the previous works, the primary contributions can be summarized as follows.

(1) To optimize planning issues and operation issues cooperatively, the operation strategy of ESUs is formulated as a fuzzy multi-objective optimization model and incorporated into the bi-level planning model, which enables an adequate consideration of ESUs operation issues and further improves the quality of planning solutions.

(2) To well address high-level uncertainties and temporal correlation related to multiple RESs, regular load demands, and EVs charging load demands simultaneously, the validity index of Davies Bouldin is introduced to develop sets of probabilistic various time-sequence scenarios with high quality and diversity.

(3) Different from traditional single economic objective model, the proposed planning model can provide a set of Pareto alternative planning schemes not only from the perspective of economy, but also from the viewpoints of reliability and green energy promotion, which enables a cleaner and more efficient ADS.

1.4 Organization of manuscript

The rest of this paper is organized as follows. In section II, after the basic framework of planning method is briefly described, the method to deal with uncertainties and the mathematical planning model are presented. Subsequently, the details about the solving methods are provided in Section III. In Section IV, the rich simulation results are analyzed and discussed in detail. Finally, several highlights and remarks are concluded in Section V.

2. MATHEMATICAL FORMULATION

The proposed cooperative planning method consists of two main parts, including the method to establish typical daily scenarios and the multi-objective, bi-level planning model, shown as Fig.1.

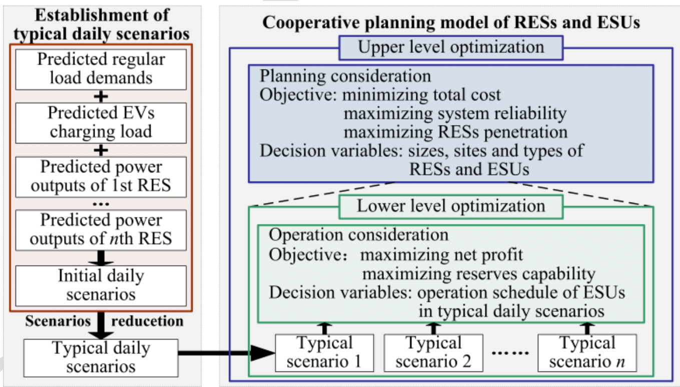

Fig. 1. Framework of optimal planning model of RESs and ESUs.

2.1 Method to establish typical scenario

This section presents the method to establish the typical daily scenarios with high quality and diversity, shown as below in detail.

2.1.1 Models of electricity energy components

The mathematical models of main components are provided as follows, including RESs, regular load demands, EVs charging load demands and ESUs.

a) Wind generators

Power outputs of WG are mainly associated with wind speed and the available power outputs can be determined by the power characteristic model of WG [26], shown as (1) to (3).

$$P_{n,t}^{\mathrm{WG}} = \begin{cases} 0, & 0 \le v_t < v_{\mathrm{ci}} \\ a + b \times v_t^3, & v_{\mathrm{ci}} \le v_t < v_{\mathrm{rated}} \\ P_n^{\mathrm{WG,rated}}, & v_{\mathrm{rated}} \le v_t < v_{\mathrm{co}} \\ 0, & v_{\mathrm{co}} \le v_t \end{cases} \tag{1}$$

$$a = \left(P_n^{\mathrm{WG,rated}} \times v_{\mathrm{ci}}^3\right) \Big/ \left(v_{\mathrm{ci}}^3 - v_{\mathrm{rated}}^3\right) \tag{2}$$

$$b = P_n^{\mathrm{WG,rated}} \Big/ \left(v_{\mathrm{rated}}^3 - v_{\mathrm{ci}}^3\right) \tag{3}$$

b) Photovoltaics

Power outputs of PV are mainly associated with the solar irradiance and the PV module conversion efficiency, and the available power outputs can be determined by the power characteristic model of PV [27], shown as (4).

$$P_{m,t}^{\mathrm{PV}} = \varepsilon^{\mathrm{PV}} \times e_t \times S_m^{\mathrm{PV}} \tag{4}$$

c) Regular load demands

To capture the time-variation feature of load demands, the chronological model proposed in IEEE-RTS system is adopted to simulate the annual normalized load demand profiles [28], where $\Delta P_{i,t}^{\mathrm{load}}$, which follows Normal distribution, denotes the random fluctuation of load demands, as given by (5).

$$P_{i,t}^{\mathrm{RL}} = P_i^{\max} \times R_w \times R_d \times R_h + \Delta P_{i,t}^{\mathrm{load}} \tag{5}$$

d) Electric vehicles charging load demands

Three vital factors are adopted to simulate uncertain EVs charging load demands, including energy demand of battery for each EV, daily arrival time, and daily departure time of each EV. Daily arrival time and departure time can be probabilistically described by Normal distributions, shown as (6) and (7), respectively [29].

$$f\left(t^{\mathrm{arr}}\right) = \begin{cases} \dfrac{1}{\sigma^{\mathrm{arr}} \times \sqrt{2\pi}} \exp\left[-\dfrac{\left(t^{\mathrm{arr}} + 24 - \mu^{\mathrm{arr}}\right)^2}{2\left(\sigma^{\mathrm{arr}}\right)^2}\right], & 0 < t^{\mathrm{arr}} \le \mu^{\mathrm{arr}} - 12 \\ \dfrac{1}{\sigma^{\mathrm{arr}} \times \sqrt{2\pi}} \exp\left[-\dfrac{\left(t^{\mathrm{arr}} - \mu^{\mathrm{arr}}\right)^2}{2\left(\sigma^{\mathrm{arr}}\right)^2}\right], & \mu^{\mathrm{arr}} - 12 < t^{\mathrm{arr}} \le 24 \end{cases} \tag{6}$$

$$f\left(t^{\mathrm{dep}}\right) = \begin{cases} \dfrac{1}{\sigma^{\mathrm{dep}} \times \sqrt{2\pi}} \exp\left[-\dfrac{\left(t^{\mathrm{dep}} - \mu^{\mathrm{dep}}\right)^2}{2\left(\sigma^{\mathrm{dep}}\right)^2}\right], & 0 < t^{\mathrm{dep}} \le \mu^{\mathrm{dep}} + 12 \\ \dfrac{1}{\sigma^{\mathrm{dep}} \times \sqrt{2\pi}} \exp\left[-\dfrac{\left(t^{\mathrm{dep}} - \mu^{\mathrm{dep}} - 24\right)^2}{2\left(\sigma^{\mathrm{dep}}\right)^2}\right], & \mu^{\mathrm{dep}} + 12 < t^{\mathrm{dep}} \le 24 \end{cases} \tag{7}$$

To obtain the data of energy demands, driving distance is simulated based on Logarithmic Normal distribution, shown as (8). Then energy demands of battery for each EV can be calculated by (9).

$$f\left(d^{\mathrm{dri}}\right) = \frac{1}{\sigma^{\mathrm{dri}} \times d^{\mathrm{dri}} \times \sqrt{2\pi}} \exp\left[-\frac{\left(\ln d^{\mathrm{dri}} - \mu^{\mathrm{dri}}\right)^2}{2\left(\sigma^{\mathrm{dri}}\right)^2}\right] \tag{8}$$

$$E_f^{\mathrm{demand}} = d_f^{\mathrm{dri}} \times W_f^{\mathrm{EV,rated}} \tag{9}$$

Then, the operating state (charging or not) of each EV can be calculated according to (10) to (11), and the collective charging load of all the EVs at time *t* can be calculated by (12).

$$P_{f,t}^{\mathrm{EV}} = \begin{cases} 0, & E_{f,t}^{\mathrm{EV}} \ge E_f^{\mathrm{demand}} \\ P_f^{\mathrm{EV,rated}}, & E_{f,t}^{\mathrm{EV}} < E_f^{\mathrm{demand}} \end{cases} \tag{10}$$

$$E_{f,t}^{\mathrm{EV}} = E_{f,t-1}^{\mathrm{EV}} + P_f^{\mathrm{EV}} \times \eta_f^{\mathrm{C}} \times \Delta t \tag{11}$$

$$P_t^{\mathrm{EV}} = \sum_{f=1}^{N_t^{\mathrm{EV}}} P_{f,t}^{\mathrm{EV}} \tag{12}$$

What needs to be pointed out is that each EV is assumed to begin to charge when it finishes the last trip of a day. Meanwhile, EV keeps being plugged into the charging piles until the scheduled departure time or that the SOC of the battery reaches a certain level.

e) Energy storage units

Although ESUs have the flexible ability to regulate active power and energy, the operation of ESUs should be strictly under the constraints of permissible range of SOC and charging/discharging power, and especially the constraints of periodical behavior, shown as (13) to (16).

$$E_{k,sc,t}^{\mathrm{ESU}} = \begin{cases} E_{k,sc,t\text{-}1}^{\mathrm{ESU}} + \eta_k^{\mathrm{C}} \times P_{k,sc,t}^{\mathrm{ESU}} \times \Delta t, & P_{k,sc,t}^{\mathrm{ESU}} \geq 0 \\ E_{k,sc,t\text{-}1}^{\mathrm{ESU}} + P_{k,sc,t}^{\mathrm{ESU}} \times \Delta t \big/ \eta_k^{\mathrm{D}}, & P_{k,sc,t}^{\mathrm{ESU}} < 0 \end{cases} \tag{13}$$

$$\sum_{t=1}^{24} \left(\eta_k^{\mathrm{C}} \times P_{k,sc,t}^{\mathrm{ESU}} + P_{k,sc,t}^{\mathrm{ESU}} \big/ \eta_k^{\mathrm{D}} \right) \times \Delta t = 0 \tag{14}$$

$$\left| P_{k,sc,\mathrm{t}}^{\mathrm{ESU}} \right| \leq P_k^{\mathrm{ESU,rated}} \tag{15}$$

$$SOC_k^{\min} \leq SOC_{k,sc,t}^{\mathrm{ESU}} \leq SOC_k^{\max} \tag{16}$$

2.1.2 Scenarios establishment and selection

After the power generations and consumptions are obtained, the typical daily scenarios can be established. The detailed process is described as follows.

a) Initial daily scenarios establishment

The annual predicted time-series profiles are normalized by their respective maximums and minimums, shown as (17). Then, these normalized annual time-dependent data are segmented into 365 daily intervals to establish the initial daily scenario matrix S^{initial}.

$$x_t^{\mathrm{nor}} = \left(x_t - x^{\min} \right) \big/ \left(x^{\max} - x^{\min} \right) \tag{17}$$

b) Typical daily scenarios selection

According to the hourly variation trends of load and RESs, these 365 daily patterns are clustered into typical daily profiles by k-means clustering. To take quality and diversity of typical scenarios into account adequately, the validity index of Davies Bouldin (I^{DB}) is adopted to determine the proper number of clustering center [30], shown as (18) to (21). Meanwhile, the number of vector in each cluster center is used to obtain the probability for each typical scenario. Thus, the matrix S^{initial} is converted to the typical daily scenario matrix S^{typical}.

$$I_{\mathrm{DB}}\left(N^{\mathrm{sc}} \right) = \sum_{g=1}^{N^{\mathrm{sc}}} \left(\max_{h=1,\ldots,N^{\mathrm{sc}}, h \neq g} R_{gh} \right) \Big/ N^{\mathrm{sc}} \tag{18}$$

$$R_{gh} = \left(S_g + S_h \right) \big/ d_{gh} \tag{19}$$

$$S_g = \sum_{x \in C_g} d\left(x, C_g \right) \Big/ N_g \tag{20}$$

$$d_{gh} = \left\| C_g - C_h \right\| \tag{21}$$

Then, the variables of matrix S^{typical} are restored to the original bounds and then adopted to represent the diverse temporal scenarios probabilistically, where high-level uncertainties and time-correlation are addressed simultaneously.

2.2 Planning problem formulation

To formulate RESs and ESUs planning problem and consider how short-terms operation can affect and be affected by long-terms planning, a hierarchical decision process is proposed with two levels of decision, shown as follows.

2.2.1 Optimization objective of upper level: long-terms planning

Different from the traditional planning, a multi-objective approach is adopted to provide different alternative planning schemes. Three objectives are considered, including the economic objective to minimize total costs, the reliability objective to minimize expected energy not supply (EENS), and the eco-friendly objective to maximize the RESP. Thus, planning schemes are provided in a sustainable manner, considering the reliability criterion of the energy supply and the economical-efficient of planning schemes simultaneously.

a) Economic objective of planning issue

The investment cost, the maintenance cost, and the operation cost constitute the economic objective function, shown as (22).

$$F_1^{\mathrm{U}} = \min\left(C_{\mathrm{d}}^{\mathrm{inv}} + C_{\mathrm{d}}^{\mathrm{mai}} + C_{\mathrm{d}}^{\mathrm{ope}}\right) \tag{22}$$

$$\begin{aligned} C_{\mathrm{d}}^{\mathrm{inv}} = {} & \frac{\delta^{\mathrm{PV}}}{365} \times \sum_{m \in \Omega_{\mathrm{PV}}} cc^{\mathrm{PV}} \times P_m^{\mathrm{PV,rated}} + \frac{\delta^{\mathrm{WG}}}{365} \times \sum_{n \in \Omega_{\mathrm{WG}}} cc^{\mathrm{WG}} \times P_n^{\mathrm{WG,rated}} \\ & + \frac{\delta_k^{\mathrm{ESU}}}{365} \times \sum_{k \in \Omega_{\mathrm{ESU}}} \left(cc_k^{\mathrm{PCS}} \times P_k^{\mathrm{ESU,rated}} + cc_k^{\mathrm{B\&R}} \times S_k^{\mathrm{ESU,rated}}\right) \end{aligned} \tag{23}$$

$$\begin{aligned} C_{\mathrm{d}}^{\mathrm{mai}} = {} & \frac{1}{365} \times \left(\sum_{m \in \Omega_{\mathrm{PV}}} cm^{\mathrm{PV}} \times P_m^{\mathrm{PV,rated}} + \sum_{n \in \Omega_{\mathrm{WG}}} cm^{\mathrm{WG}} \times P_n^{\mathrm{WG,rated}} + \sum_{k \in \Omega_{\mathrm{ESU}}} cm_k^{\mathrm{FOM}} \times P_k^{\mathrm{ESU,rated}} \right) \\ & + \sum_{k \in \Omega_{\mathrm{ESU}}} \left[\omega_{sc} \times \sum_{sc=1}^{N^{\mathrm{sc}}} \left(cm_k^{\mathrm{VOM}} \times P_k^{\mathrm{ESU,rated}} \times h_{k,sc} \right) \right] \end{aligned} \tag{24}$$

$$C_{\mathrm{d}}^{\mathrm{ope}} = \sum_{sc=1}^{N^{\mathrm{sc}}} \left(\omega_{sc} \times C_{sc}^{\mathrm{ope}} \right) \tag{25}$$

$$C_{sc}^{\mathrm{ope}} = \sum_{t=1}^{24} EP_t \times \left(P_{sc,t}^{\mathrm{TL}} - \sum_{m \in \Omega_{\mathrm{PV}}} P_{m,sc,t}^{\mathrm{PV}} - \sum_{n \in \Omega_{\mathrm{WG}}} P_{n,sc,t}^{\mathrm{WG}} \right) \times \Delta t \tag{26}$$

$$P_{sc,t}^{\mathrm{TL}} = \sum_{i \in \Omega_{\mathrm{bus}}} \left(P_{i,sc,t}^{\mathrm{RL}} + P_{i,sc,t}^{\mathrm{EV}} \right) + \sum_{l \in \Omega_{\mathrm{line}}} P_{l,sc,t}^{\mathrm{loss}} + \sum_{k \in \Omega_{\mathrm{ESU}}} P_{k,sc,t}^{\mathrm{ESU}} \tag{27}$$

$$\delta^{\mathrm{PV}} = \left[r \times (1+r)^{T^{\mathrm{PV}}} \right] \Big/ \left[(1+r)^{T^{\mathrm{PV}}} - 1 \right] \tag{28}$$

$$\delta^{\mathrm{WG}} = \left[r \times (1+r)^{T^{\mathrm{WG}}} \right] \Big/ \left[(1+r)^{T^{\mathrm{WG}}} - 1 \right] \tag{29}$$

$$\delta_k^{\mathrm{ESU}} = \left[r \times (1+r)^{T_k^{\mathrm{ESU}}} \right] \Big/ \left[(1+r)^{T_k^{\mathrm{ESU}}} - 1 \right] \tag{30}$$

$$P_{l,sc,t}^{\mathrm{loss}} = I_{l,sc,t}^2 \times R_l \tag{31}$$

b) Reliability objective of planning issue

To minimize EENS serves as the second objective, shown as (32). To take the influences of RESs and ESUs on reliability into account adequately, the fluctuant power outputs and the chronological contingencies of RESs and ESUs are investigated based on the analytical method proposed in [31]. The two-state Markov process model serves to simulate sequence transitions between operative states and failed states of main components, including WGs, PVs, ESUs and feeders.

$$F_2^{\mathrm{U}} = \min\left[\sum_{sc=1}^{N^{\mathrm{sc}}}\left(\omega_{sc}\times I_{sc}^{\mathrm{EENS}}\right)\right] \tag{32}$$

$$I_{sc}^{\mathrm{EENS}} = \sum_{sy=1}^{N^{\mathrm{sy}}}\left(I_{sy,sc}^{\mathrm{EENS}}\right)\Big/N^{\mathrm{sy}} \tag{33}$$

c) Eco-friendly objective of planning issue

RESP is adopted to represent the eco-friendly performance. Thus, to maximize the RESP serves as the third objective for the planning issue, shown as (34) to (36).

$$F_3^{\mathrm{U}} = \max\left(Pen_{\mathrm{d}}^{\mathrm{RES}}\right) = \max\sum_{sc=1}^{N^{\mathrm{sc}}}\left(\omega_{sc}\times Pen_{sc}^{\mathrm{RES}}\right) = \max\sum_{sc=1}^{N^{\mathrm{sc}}}\left[\omega_{sc}\times\left(W_{sc}^{\mathrm{RES}}/W_{sc}^{\mathrm{TL}}\right)\right] \tag{34}$$

$$W_{sc}^{\mathrm{RES}} = \sum_{t=1}^{24}\left(\sum_{m\in\Omega_{\mathrm{PV}}}P_{m,sc,t}^{\mathrm{PV}} + \sum_{n\in\Omega_{\mathrm{WG}}}P_{n,sc,t}^{\mathrm{WG}}\right)\times\Delta t \tag{35}$$

$$W_{sc}^{\mathrm{TL}} = \sum_{t=1}^{24}\left(P_{sc,t}^{\mathrm{TL}}\times\Delta t\right) \tag{36}$$

2.2.2 Objective function of lower level: short-terms operation

In this paper, it is assumed that ESUs are invested by distribution company, and thereby the arbitrage increase and the reliability improvement are adopted to formulate the operation strategy of ESUs.

a) Economic objective of operation issue

Distribution company can obtain extra arbitrage according to TOU electricity prices during different hours. Thus, to maximize the arbitrage is adopted to be the economic objective, shown as (37).

$$F_1^{\mathrm{L}} = \max\left(\pi_{k,sc}^{\mathrm{ESU}}\right) = \max\left[\sum_{t=1}^{24}EP_t\times\left(-P_{k,sc,t}^{\mathrm{ESU}}\right)\times\Delta t\right] \tag{37}$$

b) Reliability objective of operation issue

When faults occur, ESUs can provide some degree of power supply to essential loads and participate in the service restoration. To investigate the effects of ESUs on reliability improvement, the reserve capability is introduced to represent the maximum power output that the ESU can supply to the ADS under all operative constraints, shown as (38). Thus, to maximize the reserve capability is adopted to be another operation objective, shown as (39).

$$P_{k,sc,t}^{\mathrm{ESU,ava}} = \min\left\{P_k^{\mathrm{ESU,rated}}, \left[\left(SOC_{k,sc,t\text{-}1}^{\mathrm{ESU}} - SOC_k^{\min}\right)\times S_k^{\mathrm{ESU,rated}}\times\eta_k^{\mathrm{D}}\right]\Big/\Delta t\right\} \tag{38}$$

$$F_2^{\mathrm{L}} = \max\left[\sum_{t=1}^{24}P_{k,sc,t}^{\mathrm{ESU,ava}}\Big/24\right] \tag{39}$$

Obviously, these two proposed objectives are inconsistent in some extent; the increase of reserve capability would be at the cost of capacity of ESUs to execute economic dispatch. Furthermore, it is worthy to mention that, in terms of bi-level programming, no multiple optima can be allowed in lower level. Therefore, the unique optimal solution must be obtained in lower level. To address this problem, the fuzzy satisfaction maximizing method based on fuzzy mathematic theory is adopted to address this multi-objective problem and get the most balanced solution [32]. Thus, to maximize the fuzzy satisfaction function is adopted as the objective function in lower level, shown as (40). A bigger value of it implies a higher fuzzy satisfaction value and indicates a better operation schedule.

$$F_{\mathrm{fuzzy}}^{\mathrm{L}} = \max\left(\mu^{\mathrm{L}}\right) \tag{40}$$

$$\mu^{\mathrm{L}} = \min\left\{\mu\left(F_1^{\mathrm{L}}\right),\ \mu\left(F_2^{\mathrm{L}}\right)\right\} \tag{41}$$

2.2.3 Constraints

This section presents the important constraints that must be obeyed, shown as follows.

a) Installed capacity constraints

In order to alleviate the undesirable impacts brought by the bi-directional power flow, the integration proportion of RESs should be smaller than a permissible value, shown as (42).

$$\sum_{m\in\Omega_{\mathrm{PV}}} P_m^{\mathrm{PV,rated}} + \sum_{n\in\Omega_{\mathrm{WG}}} P_n^{\mathrm{WG,rated}} \le \lambda^{\mathrm{I}} \times S^{\mathrm{sub}} \tag{42}$$

b) Operation constraints of network

Operation constrains of networks are shown as (43) to (46), including power flow equations, and security constraints of current and voltage.

$$P_{i,sc,t} = U_{i,sc,t} \times \sum_{i,j\in\Omega_{\mathrm{bus}}} U_{j,sc,t} \times \left(G_{ij} \times \cos\theta_{ij,sc,t} + B_{ij} \times \sin\theta_{ij,sc,t} \right) \tag{43}$$

$$Q_{i,sc,t} = U_{i,sc,t} \times \sum_{i,j\in\Omega_{\mathrm{bus}}} U_{j,sc,t} \times \left(G_{ij} \times \sin\theta_{ij,sc,t} - B_{ij} \times \cos\theta_{ij,sc,t} \right) \tag{44}$$

$$U_{i,sc,t}^{\min} \le U_{i,sc,t} \le U_{i,sc,t}^{\max} \tag{45}$$

$$\left| I_{l,sc,t} \right| \le I_l^{\max} \tag{46}$$

c) Operation constraints of energy storage units

As mentioned in Section 2.1.1, the operation of ESUs should be strictly under the constraints shown as (13) to (16).

3. OPTIMIZATION METHODS FOR PLANNING MODEL

The proposed model is a problem of multi-objective, bi-level, multi-constraint, nonlinear optimization with mixed-integers. In view of the good performances of PSO to solve nonlinear, multi-extrema optimization problems, PSO is adopted to solve this proposed planning problem. In this section, the optimization method including solving algorithm and solving flow are presented in detail as follows.

3.1 Solving algorithms

To satisfy the requirement of bi-level programming problem, Pareto-based multi-objective PSO (MOPSO) and fuzzy MOPSO are adopted to solve upper level and lower level respectively according to different features of them. Furthermore, to improve the optimization performance, several modified measures are adopted, shown as follows.

a) Tent chaotic mapping

In the beginning of the standard PSO, the initial population of particles is generated randomly. However, it is easily to suffer from pseudo-random number sequence [32]. Therefore, the tent chaotic mapping with the merits of ergodicity and randomness is employed in this modified PSO to generate the initial population.

b) Fast non-dominated sorting approach

To obtain a set of planning solutions with diversity and in converging near the Pareto optimal front, the fast non-dominated sorting approach is adopted in this modified PSO, which is introduced in Fast Non-dominated Sorting Genetic Algorithm (NSGA-II) [33]. Meanwhile, the global best solution in each iteration is selected according to the crowding-distance assignment of each non-dominated solution.

3.2 Solving flow

In the beginning, the initial population of upper level is generated by tent mapping. Then, each particle of upper level, representing an allocation scheme of RESs and ESUs, is sent to the lower level. The short time scale OPF is executed by fuzzy MOPSO to optimize the schedules of all the ESUs, which are fed back to upper level to calculate the objectives of this corresponding candidate allocation scheme for the upper level. The same steps are iterated until Pareto-based MOPSO in the upper level converges, shown as Fig. 2.

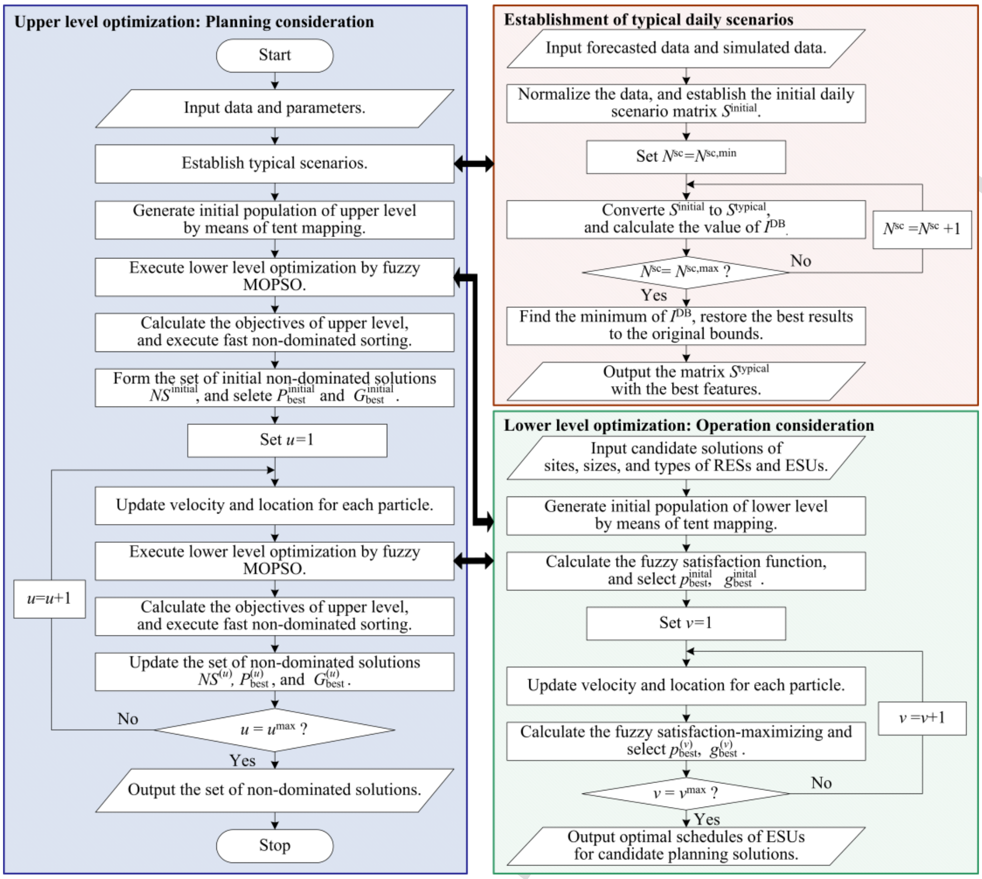

Fig. 2. Optimization procedure of finding optimized planning schemes.

4. CASE STUDY

This section presents the case studies, which are implemented in the Matlab®2017 programming environment using a computer with an Intel®Core i5 processor, 3.10 GHz CPU and 8 GB of RAM.

4.1 Description

In order to verify effectiveness and feasibility, the proposed planning model and optimization methods are applied to solve different simulation studies based on PG&E-69 bus distribution system and IEEE-33 bus distribution system. The topologies of these two benchmark systems are provided in Fig.3, where candidate locations of WGs, PVs, and ESUs are marked, respectively. What needs to be pointed out is that these candidate locations are selected according to the installation condition constraints such as the geographical conditions, landscape aesthetics constraints without considering other technical constraints.

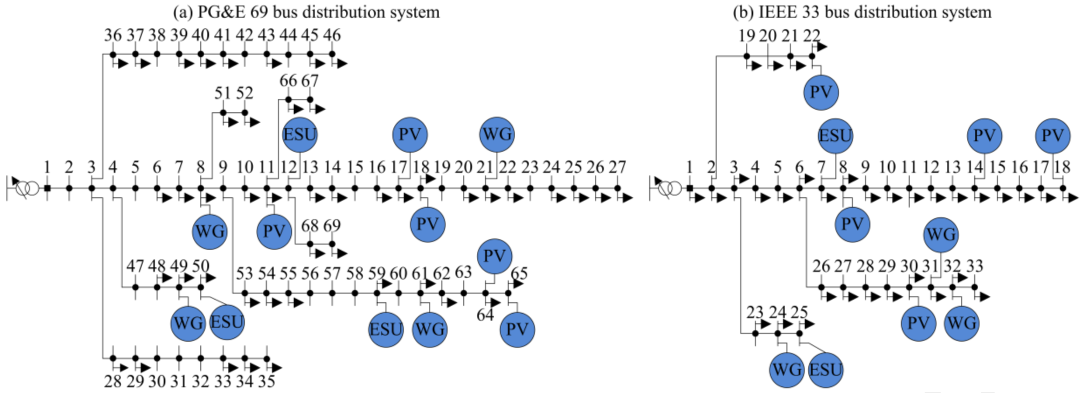

Fig. 3. PG&E-69 bus and IEEE-33 bus benchmark distribution systems.

The voltage base for these two benchmark systems is 12.6kV, and other detailed data can be found in the references [34] and [35], respectively. The failure rate and repair time for each feeder are 0.49 fail/km per year and 2 hour/fail, respectively.

In terms of WGs, the cut-in wind speed, rated wind speed, and cut-out wind speed are 3.5m/s, 12m/s, and 25m/s, respectively [36]. In terms of PVs, the Yingli n-PERT PANDA cells are adopted in this work, of which the module efficiency can reach to 20.1%. The rated power and the area of per panel are 0.33kW and 1.6447m^2, respectively [37]. Other technical and economic parameters of RESs and three types of ESUs are provided in Table 1 and Table 2, respectively.

Table 1. Technical and economic parameters of RESs [38].

	Capital cost	O&M cost	Lifetime	MTTF	MTTR
WGs	1220($/kW)	33 ($/kW)	20 (yr)	1920 (h)	80 (h)
PVs	2100($/kW)	16 ($/kW)	25 (yr)	1920 (h)	80 (h)

Table 2. Technical and economic parameters of ESUs [39].

	LAB	LIB	NaS
PCS ($/kW)	380	459	371
Storage section ($/kWh)	311	789	327
Fixed O&M ($/kW)	3.89	5.78	3.89
Variable O&M ($/MWh)	0.43	1.16	0.35
Efficiency (%)	0.80	0.90	0.85
Range of SOC (%)	30~70	20~80	10~90
Lifetime (yr)	10	12.5	15

Meanwhile, taking the load simultaneity factor into account, it is assumed that there are 1500 residents in these two distribution systems. According to the U.S. national household travel survey, car ownership for per household equals to 1.86 [40]. The penetration of EVs is 20 percent, and the average charging frequency for each EV is set to 0.65 per day. The technical parameters of battery used in four types of EVs, and probability distribution parameters of charging time and driving distance are provided in Table 3 and Table 4, respectively.

Table 3. Technical parameters of battery used in EVs [41].

	Citroë C Zero	BMW i3	Nissan Leaf	BYD E6
Charging power rating(kW)	3.7	3.7	3.7	7
Battery capacity(kWh)	14.5	22	24	60
Energy consumption(kWh/km)	0.179	0.179	0.153	0.209
Efficiency(%)	90	90	90	90
Proportion(%)	15	30	35	20

Table 4. Probability distribution parameters of EVs charging time and driving distance.

	Arrival time		Departure time		Driving distance	
	μ^{arr}	σ^{arr}	μ^{dep}	σ^{dep}	μ^{dri}	σ^{dri}
Weekdays	18	3	7	3	4.79	1.84
Weekends	15	6	9	6	5.43	2.46

The TOU electricity prices are provided in Fig. 4. The interest rate equals to 8% [42].

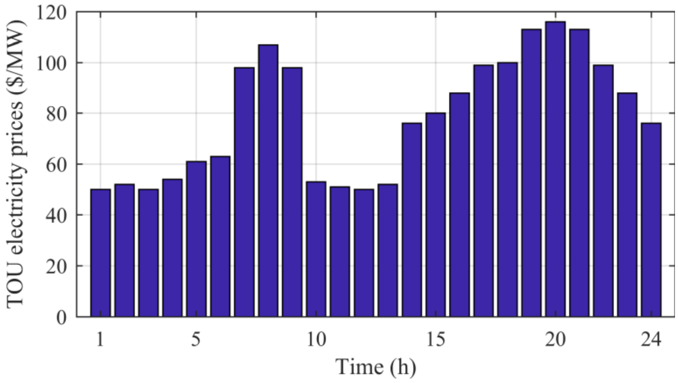

Fig. 4. TOU electricity prices.

To investigate the influences brought by ESUs and EVs on the planning schemes, three different cases are studied for each system. The arrangements of these three cases are shown in Table 5.

Table 5. Case study arrangements.

	RESs	ESUs	EVs	Model
Case 1	√	×	√	Upper level planning model alone
Case 2	√	√	×	Proposed bi-level model
Case 3	√	√	√	Proposed bi-level model

To ease computational burden, it is assumed that the atmospheric conditions are similar in these candidate locations for RESs. Fig.5 (a) and Fig.5 (b) provide annual wind speed and solar irradiance, respectively. The profiles of regular load demands shown in Fig.5 (c) are extracted in IEEE-RTS. To take uncertainties of EVs charging load demands into account, sequential Monte Carlo Simulation is adopted to simulate EVs charging behaviors, shown as Fig.5 (d).

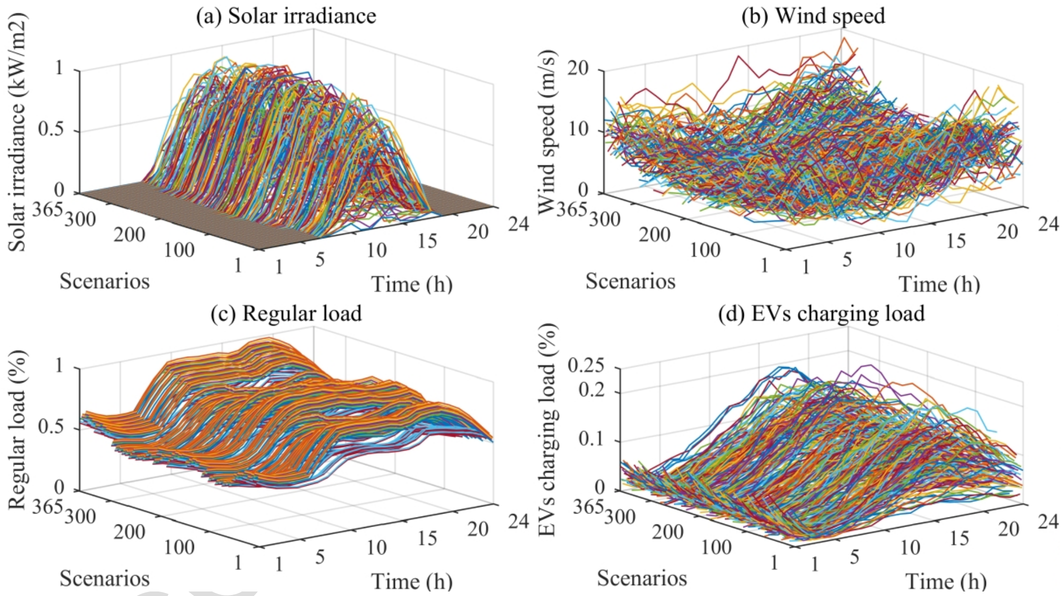

Fig. 5. Annual data of wind speed, solar irradiance, load demands and EV charging demand.

To analyze different influences between regular load demands and EVs charging load demands contrastively, required electricity demands for these three cases are equal in amount. Thus, in Case 2, the equivalent load is introduced to denote the same required electricity demands as EVs charging load demands and has the same variation trend as regular load demands.

4.2. Results of typical daily scenarios

Considering the balance between computational burden and accuracy of planning calculation, the number of cluster center is determined by I^{DB} in the interval of [2, 50], shown as Fig.6. The corresponding typical daily scenarios with high quality and diversity are illustrated in Fig.7.

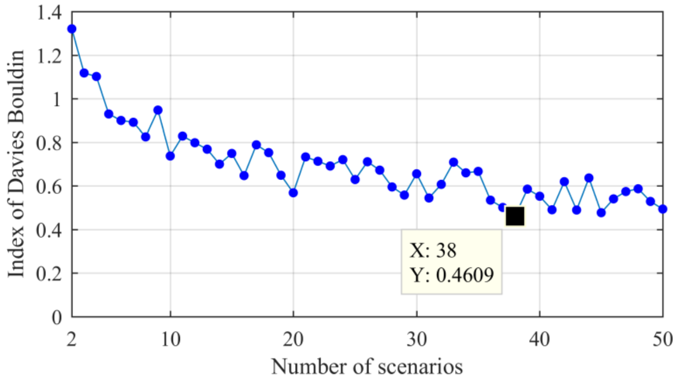

Fig. 6. Variation trend of index of Davies Bouldin.

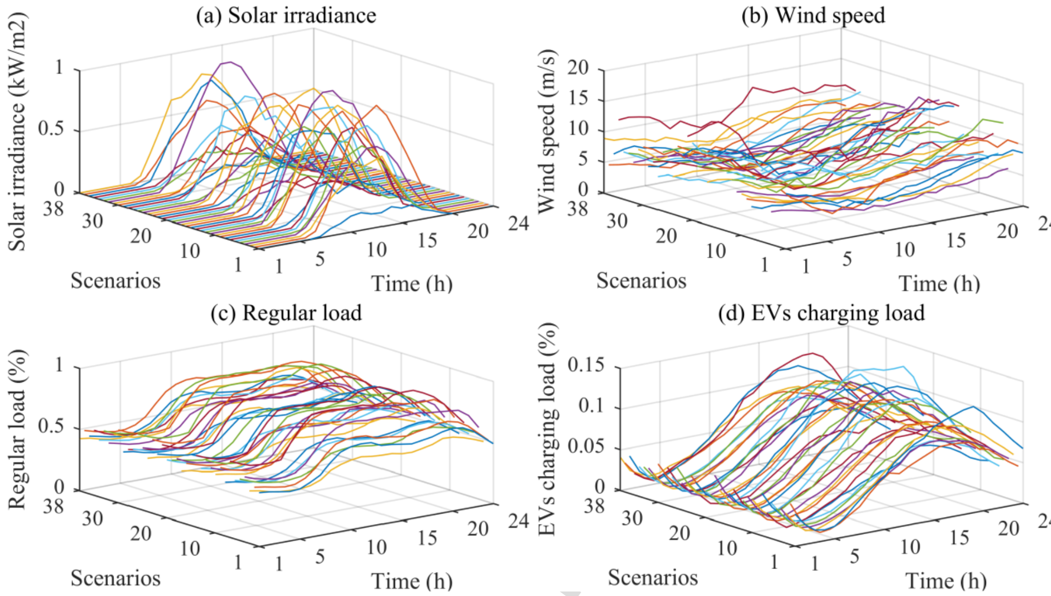

Fig. 7. Typical scenarios of solar irradiance, wind speed, load demands and EV charging demands.

To illustrate the influences on the total load demands brought by EVs charging load demands, the curves of different load demands in several typical daily scenarios are provided in Fig.8.

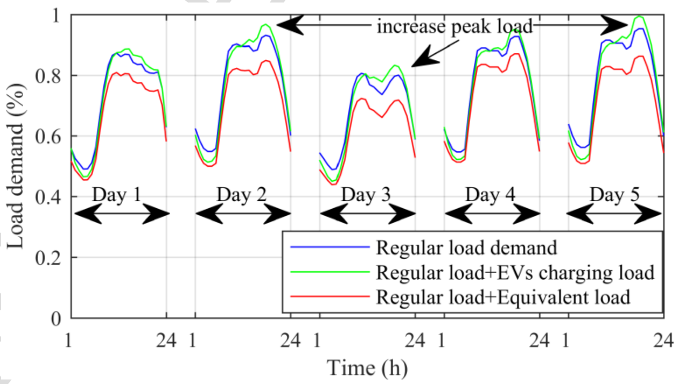

Fig. 8. Curves of load demands in different Cases.

As shown in Fig.8, although charging habit and travel demand of each EV are highly uncertain, the aggregate load demands of EVs charging are of obvious feature with time. Meanwhile, comparing with the equivalent load, EVs charging load demands increase the peak load obviously, which will result in load congestion and reliability decrease.

4.3. Results of planning problem

In each case, ten alternative non-dominated solutions are provided for decision makers, shown as Fig. 9. The decision makers have the flexibility to choose the appropriate planning schemes according to their different planning targets, including economy, reliability, and environment for each case.

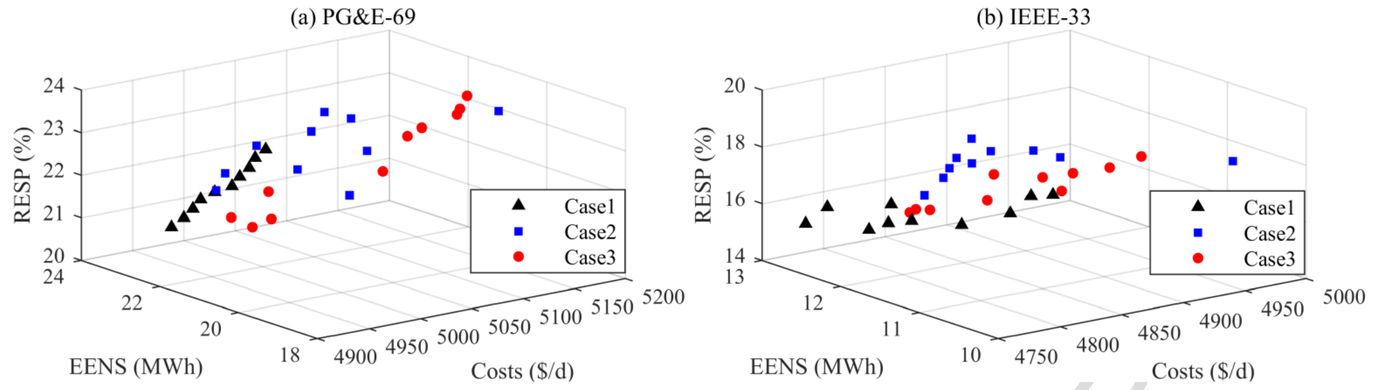

Fig. 9. Alternative non-dominated solutions in different cases.

In order to appraise the performance of the adopted solving strategy, Set Coverage metric (C-metric) is adopted to compare the performances of modified MOPSO with standard multiple objective differential evolution algorithm (MODE) and standard MOPSO. As shown by (47), C-metric is defined as the percentage of the solutions in B that are dominated by at least one solution in A [43].

$$C(A,B)=\frac{\left|\{y\in B\mid \exists x\in A: x \text{ dominate } y\}\right|}{|B|} \tag{47}$$

C-metric can judge the dominant relationship between two sets of Pareto solutions, and therefore it has been perceived to be one of the most vital indexes to assess the performances of different solving solutions. The provided results in Table 6 show that most of the non-dominated solutions obtained by modified MOPSO dominate the solutions obtained by the other ones, which indicates the priority of the adopted solving strategy.

Table 6. Average set coverage between modified MOPSO, standard MODE and standard MOPSO.

C-metric	PG&E-69			IEEE-33		
	Case 1	Case 2	Case 3	Case 1	Case 2	Case 3
C(modified MOPSO, standard MODE)	50%	40%	40%	30%	70%	70%
C(standard MODE, modified MOPSO)	30%	20%	10%	20%	20%	10%
C(modified MOPSO, standard MOPSO)	50%	50%	60%	40%	40%	50%
C(standard MOPSO, modified MOPSO)	10%	10%	20%	10%	10%	20%

4.4. Discussion and analyses

To compare and analyze the whole conditions of different cases, the box-and-whisker plots of different solutions are provided in Fig.10. Meanwhile, the average values of these objectives for different cases are provided in Table 7.

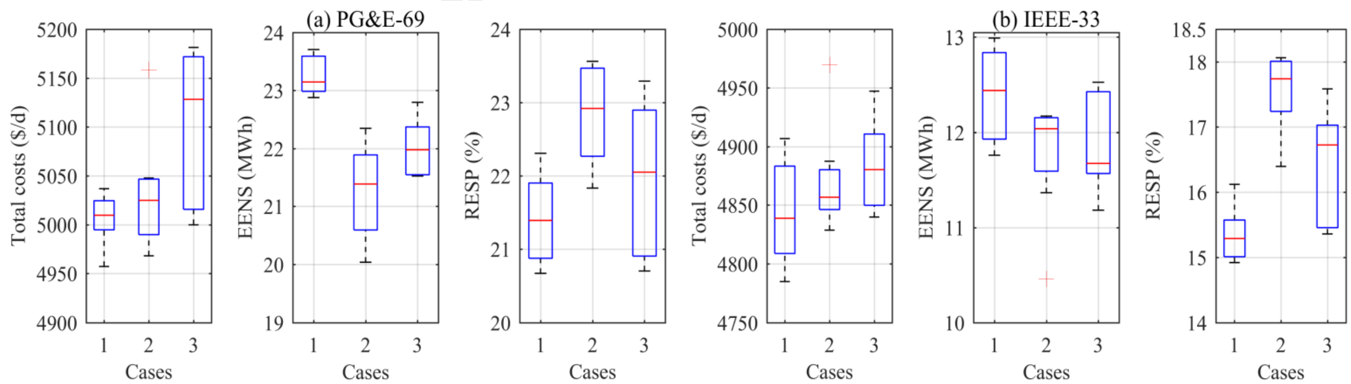

Fig. 10. Box-and-whisker plots of non-dominated solutions in different cases.

Table 7. Average values of objectives for different cases.

	PG&E-69			IEEE-33		
	Case 1	Case 2	Case 3	Case 1	Case 2	Case 3
Cost ($/d)	5007.16	5027.92	5097.59	4844.08	4868.79	4882.18
EENS (MWh)	23.2515	21.2752	22.0198	12.4010	11.7902	11.8349
RESP (%)	21.4185	22.8293	22.0120	15.3970	17.5665	16.5286

By the comparisons between Case 2 and Case 3, it can be indicated the influences of EVs charging load demands on these planning schemes. As the results show, the integration of EVs increases the total costs of ADSs, and the utilization level of RESs decreases at the same time. Furthermore, the increase of EENS also indicates that the integration of EVs reduces the reliability of system. Meanwhile, by the comparisons between Case 1 and Case 3, it also can be found out that the integration of ESUs increases total costs, however the reliability and the utilization of RESs are improved at the same time. This can be valuable from technical and the environmental viewpoints.

To discuss planning results further, the fuzzy satisfaction-maximizing method is adopted to select the most balanced solution for each case. The corresponding cost items, reliability indexes, and the values of RESP are demonstrated in Table 8. Moreover, the corresponding optimal sites, sizes and types of RESs and ESUs are also provided, respectively.

Table 8. Well balanced optimal solutions of different cases.

	PG&E-69			IEEE-33		
	Case 1	Case 2	Case 3	Case 1	Case 2	Case 3
Cost items ($/d)	4957.27	5009.48	5017.88	4866.91	4887.55	4890.58
Inv. & Mai.	976.50	1293.78	1281.69	625.68	812.55	747.10
Operation cost	3980.77	3715.70	3737.09	4241.23	4075.00	4143.48
EENS (MWh)	23.19	20.03	22.35	12.29	11.36	11.64
RESP (%)	20.75	22.23	20.90	14.92	17.97	16.98
WG (MW)	Bus08: 0.05 Bus21: 0.10 Bus49: 0.35 Bus61: 1.20 Total: 1.70	Bus08: 0.00 Bus21: 0.10 Bus49: 0.35 Bus61: 1.20 Total: 1.65	Bus08: 0.05 Bus21: 0.10 Bus49: 0.30 Bus61: 1.20 Total: 1.65	Bus24: 0.30 Bus31: 0.20 Bus32: 0.20 Total: 0.70	Bus24: 0.50 Bus31: 0.20 Bus32: 0.30 Total: 1.00	Bus24: 0.50 Bus31: 0.20 Bus32: 0.30 Total: 1.00
PV (MW)	Bus11: 0.00 Bus17: 0.05 Bus18: 0.025 Bus64: 0.125 Bus65: 0.05 Total: 0.25	Bus11: 0.025 Bus17: 0.050 Bus18: 0.050 Bus64: 0.225 Bus65: 0.050 Total: 0.40	Bus11: 0.125 Bus17: 0.050 Bus18: 0.050 Bus64: 0.150 Bus65: 0.050 Total: 0.425	Bus08: 0.05 Bus14: 0.10 Bus18: 0.10 Bus22: 0.00 Bus30: 0.15 Total: 0.40	Bus08: 0.05 Bus14: 0.00 Bus18: 0.10 Bus22: 0.10 Bus30: 0.10 Total: 0.35	Bus08: 0.10 Bus14: 0.00 Bus18: 0.10 Bus22: 0.05 Bus30: 0.05 Total: 0.30
ESU (MW; MWh)	--	Type: NaS Bus12: 0.10; 0.30 Bus50: 0.35; 1.050 Bus59: 0.10; 0.30 Total: 0.55; 1.650	Type: NaS Bus12: 0.10; 0.30 Bus50: 0.20; 0.80 Bus59: 0.10; 0.30 Total: 0.40; 1.4	--	Type: NaS Bus07: 0.10; 0.40 Bus25: 0.15; 0.60 Total: 0.25; 1.00	Type: NaS Bus07: 0.10; 0.40 Bus25: 0.10; 0.40 Total: 0.20; 0.80

A comparison between Case 1 and Case 3 is drawn when ESUs are integrated, it can be seen that the diurnal Inv. & Mai. costs experience an increase from 976.50$/d to 1281.69$/d for PG&E-69 system and from 625.68$/d to 747.10$/d for IEEE-33 system, respectively. However, it can be found that the operation costs decrease due to the more share of RESs and the extra arbitrage brought by ESUs. It reveals the monetary benefits brought by the optimal operation of ESUs. Furthermore, the improvement of reliability and the promotion of clean energy brought by ESUs are validated again by the decrease of EENS and the increase of RESP, respectively.

It is also interesting to note that the selected types of ESUs are NaS in both Case 2 and Case 3 for these two systems. It indicates that, comparing with LiB and LAB, NaS has a more advanced techno-economic performance under the current circumstances.

From the comparisons between Case 2 and Case 3, it also can be found that although the Inv. & Mai. costs decrease from 1293.78$/d to 1281.69$/d for PG&E-69 system and from 812.55$/d to 747.10$/d for IEEE-33 system, the operation costs increase from 3715.70$/d to 3737.09$/d for PG&E-69 system and from 4075.00$/d to 4143.48$/d for IEEE-33 system, respectively. It is because that the integration of EVs leads to higher peak electricity demands in Case 3. Meanwhile, it also leads to a lower system reliability, indicated by the increase of EENS. Furthermore, the utilization levels of RESs, depicted by RESP, decease from 22.23% to 20.90% for PG&E-69 system and from 17.97% to 16.98% for IEEE-33 system, respectively. An important reason for these conditions is that the EVs changing load demands further deteriorate the mismatch between power consumptions of load demands and power outputs of RESs.

Here, Mann-Kendall non-parametric correlation coefficient is adopted to investigate the mismatch between power outputs of RESs and power consumptions of load demands further. Mann-Kendall correlation coefficient is an effective tool to analyze cross-correlations between two simultaneously non-stationary time series and has been successfully applied in data analysis.

The value of Mann-Kendall correlation coefficient varies from -1 to 1, where the signal denotes the positive or negative direction of the correlation relationship and the magnitude implies the strength of the relation between the two sets of variables. The variations of Mann-Kendall correlation coefficient are provided in Fig. 11 to demonstrate the aforementioned mismatch under different circumstances.

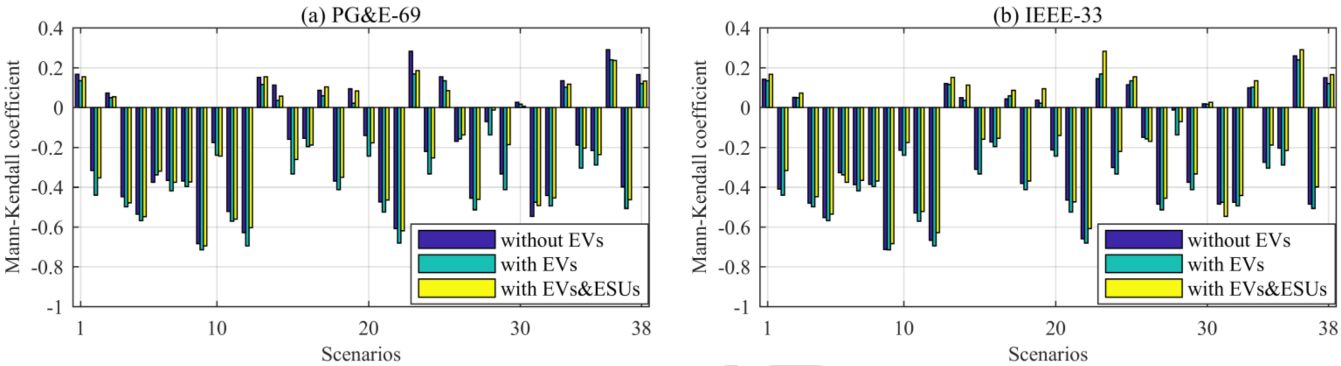

Fig. 11. Correlation coefficient between outputs of RESs and consumptions of load demands.

In Fig. 11, it is can be found that the values of Mann-Kendall correlation coefficient are smaller than zero in most scenarios, which implies that the power outputs of RESs have a negative relation with power consumptions of load demands. Furthermore, with the integration of EVs, the expected value of correlation coefficient for these 38 scenarios decreases from -0.2952 to -0.3959. These smaller values with EVs in different scenarios also verify that the EVs charging load demands deteriorate the mismatch condition. The hosting capacity for RESs decreases accordingly. Meanwhile, it is also can be found that the optimal operation of ESUs has the ability to ameliorate this undesirable condition; the expected values of correlation coefficient increase to -0.1996 (PG&E-69 system) and -0.2317 (IEEE-33 system), respectively.

In order to illustrate these operation conditions, Fig.12 and Fig. 13 provide different operation profiles in two most likely scenarios and two most unlikely scenarios, respectively. The power outputs supplied by PVs, WGs, and the substation as well as corresponding power consumptions of regular load, EVs, and network losses are demonstrated clearly.

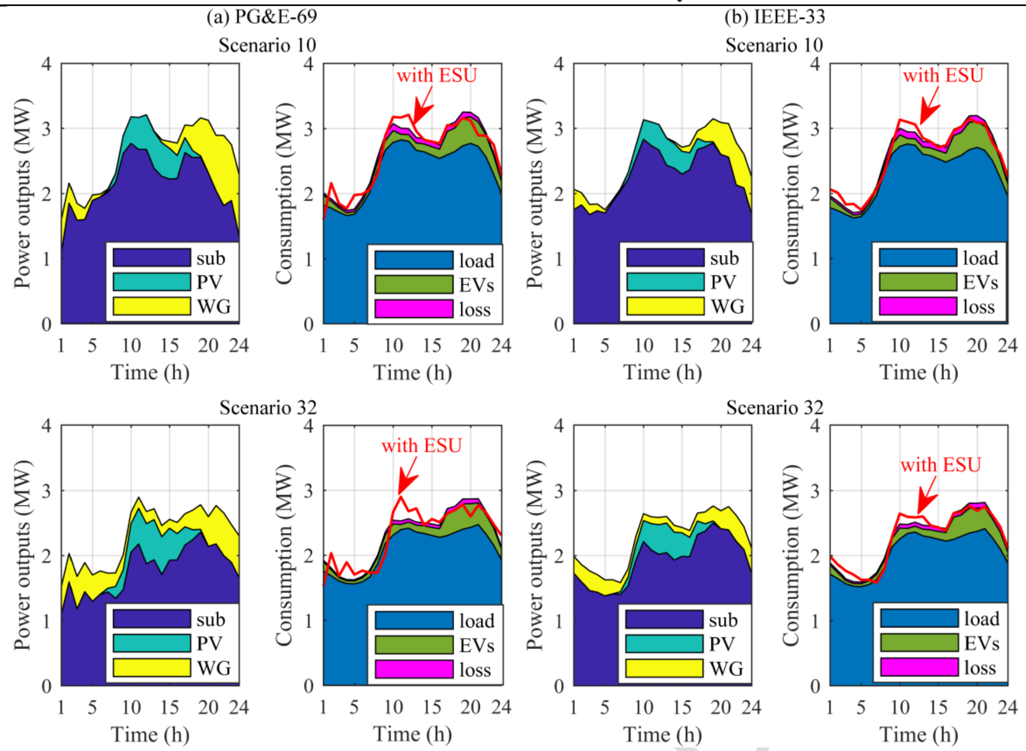

Fig. 12. Energy profiles of power outputs and load demands of the most likely scenarios.

As indicated by Fig.12, it can be observed that power outputs of PVs and WGs can complement each other well in these two scenarios, where values of RESP are promoted. The expectation of Mann-Kendall correlation coefficient between PVs and WGs for these 38 scenarios equals to -0.632, which means an obvious complementarity between these two kinds of variable RESs. In terms of power consumptions, EVs charging load demands increase the peak load demands significantly during 18h to 22h. This is the main reason why operation costs increase, shown in Table 8.

As shown in Fig. 13, the values of RESP increase significantly. RESs share more than 30% load demands in these two scenarios. Nevertheless, due to the low probability of them, the expectation values of RESP in Case 3 keep at 20.90 percent level for PG&E-69 system and 16.98 percent level for IEEE-33 system, respectively.

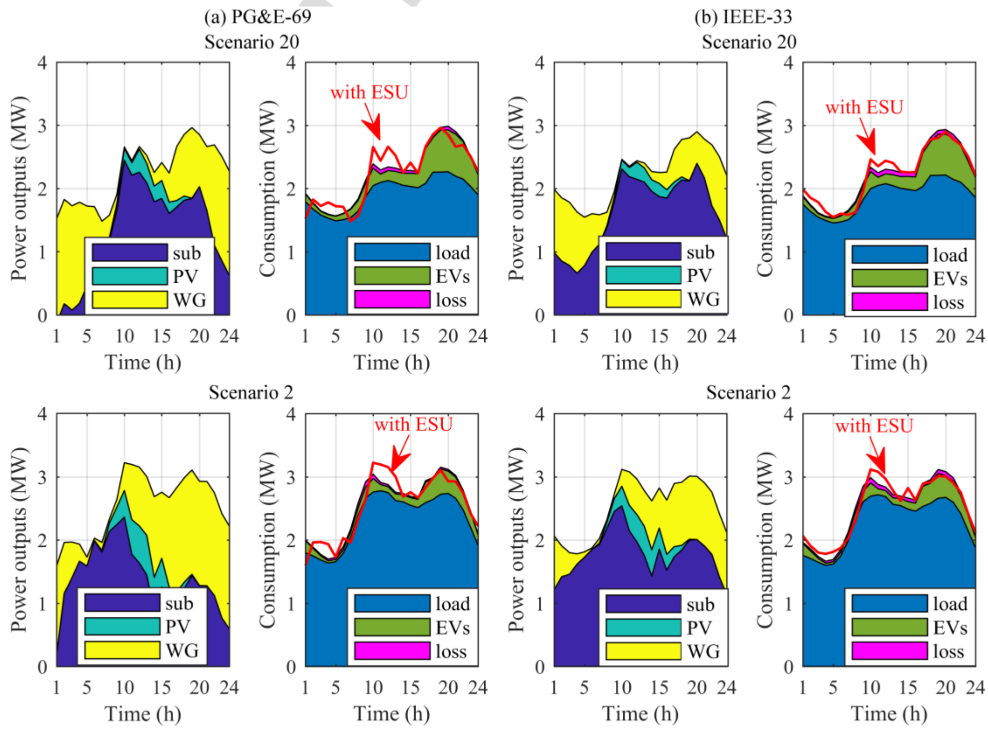

Fig. 13. Energy profiles of power outputs and load demands of the most unlikely scenarios.

Furthermore, it is can be found that optimal operation of ESUs, to some extent, has the ability to ameliorate the undesirable condition, but the effects are less marked in these scenarios. Several reasons result in the indistinctive effects, including the operation constraints, limited power ratings, and limited capacities of ESUs. Furthermore, the operation objective to improve reliability also makes ESUs keep their SOC at a certain degree to deal with possible emergencies. The operation conditions of ESUs in several scenarios are provided in Fig. 14 and Fig.15.

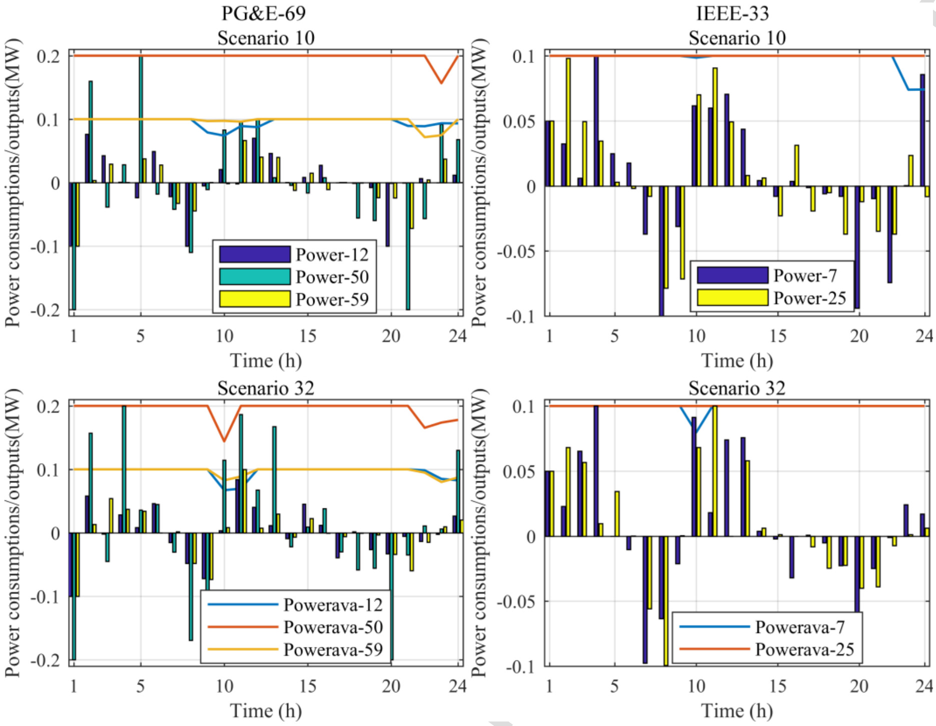

Fig. 14. Operation profiles of ESUs in the most likely scenarios.

As shown in Fig. 14, ESUs allocated in different buses all keep charging during the off-peak periods of electricity prices and discharging during the peak periods of electricity prices. Meanwhile, the reserve capabilities of these ESUs depicted by these full lines also can keep in a high degree. Thus, ESUs can take some degree of responsibility for system support when a contingency happens. Accordingly, the improvement effect of ESUs on hosting capacity for RESs further enhance the system reliability, shown as the comparison between Case 1 and Case 3 in Table 8.

Furthermore, Fig.15 demonstrates that, in spite of different operation conditions and allocation schemes, the SOC values of ESUs always stay in a reasonable range to avoid over-charge and over-discharge. Meanwhile, there are only two cycles of charge and discharge. Thus, to some extent, the lifetimes of ESUs will be conserved.

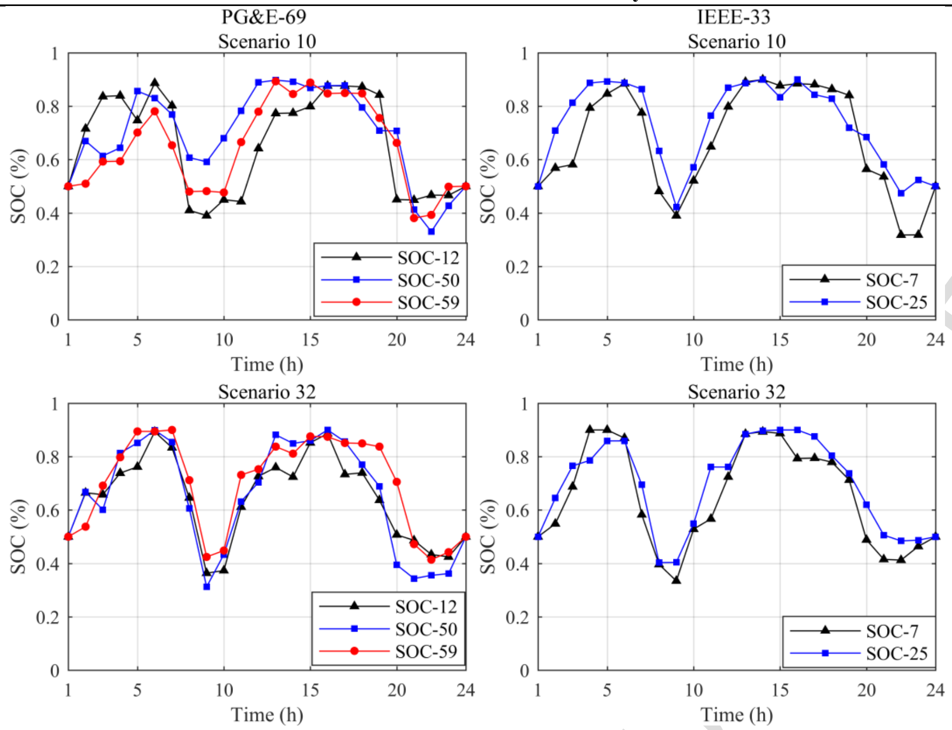

Fig. 15. SOC variations of ESUs in different scenarios.

From the above discussions, the undesirable influences of EVs charging load demands and beneficial effects of ESUs are well demonstrated from different perspectives. It also well indicates that the proposed planning model has the ability to integrate time-dependence optimal operation schedules of ESUs into planning issues, and take time-variable nature and uncertainties related with RESs and load demands into account adequately at the same time.

5. CONCLUSIONS

In this paper, a cooperative planning model between RESs and ESUs in ADSs is proposed based on multi-objective, bi-level programming. Various temporal operation scenarios with diversity and representativeness are established considering high-level uncertainties related to different kinds of RESs, regular load demands, and EVs charging load.

Simulation results verify the efficiency and feasibility of the proposed planning model and optimization methods. It is also shown that the proposed planning model incorporates the optimal operation strategy of ESUs and various operation conditions of RESs into the planning process adequately, which allows the obtained planning solutions to be more committed with reality. Meanwhile, further analyses indicate the priority of cooperative planning between RESs and ESUs compared to individual planning of RESs. Hence, based on the proper allocation and optimal operation, ESUs is an effective and feasible way to improve economy efficiency, reliability, and eco-friendly level.

Furthermore, as shown in discussion, EVs charging load demands bring about the problem of peak load increase and aggravate the mismatch between power generations of RESs and power consumptions of load demands. But to some extent, these undesirable influences can be alleviated by the optimal allocation and operation of ESUs.

As a future work, the proposed planning model and optimization methods will be applied to more actual systems. More important, to improve the planning model further, two valuable issues that the game relationship between multiple stakeholders in the electricity market environment and the lifetime models of ESUs and RESs will be taken into consideration adequately in later works.

ACKNOWLEDGEMENTS

This work was supported by the National Key Research and Development Program of China (Grant numbers：2018YFB0905203).

REFERENCES

[1] Mathiesen B V, Lund H, Karlsson K. 100% Renewable energy systems, climate mitigation and economic growth. Appl Energy 2011;88(2):488-501.

[2] Batas-Bjelic I, Rajakovic N, Duić N. Smart municipal energy grid within electricity market. Energy 2017;137:1277-85.

[3] Pillai J R, Heussen K, Østergaard P A. Comparative analysis of hourly and dynamic power balancing models for validating future energy scenarios. Energy 2011;36(5):3233-43.

[4] Morel J, Obara S, and Morizane Y. Operation strategy for a power grid supplied by 100% renewable energy at a cold region in Japan. J Sustain Dev Energy Water Environ Syst 2014;2(3):270-83.

[5] Fedak W, Anweiler S, Ulbrich R, and Jarosz B. The concept of autonomous power supply system fed with renewable energy sources. J Sustain Dev Energy Water Environ Syst 2017;5(4):579-89.

[6] Lund H, Alberg Østergaard P, Connolly D, Vad Mathiesen B. Smart energy and smart energy systems. Energy 2017;137:556-65.

[7] Soares T, Bessa R J, Pinson P, Morais H. Active distribution grid management based on robust AC optimal power flow. IEEE Trans Smart Grid. https://doi.org/10.1109/tsg.2017.2707065 [in press].

[8] Zhao J, Wang C, Zhao B, Lin F, Zhou Q, Wang Y. A review of active management for distribution networks: current status and future development trends. Electr Power Comp Syst 2014;42(3-4):280-93.

[9] Pilo F, Celli G, Ghiani E, Soma G G. New electricity distribution network planning approaches for integrating renewable. Wiley Interdiscip Rev Energy Environ 2013;2(2):140-57.

[10] Zhang J, Fan H, Tang W, Wang M, Cheng H, Yao L. Planning for distributed wind generator under active management mode. Int J Electr Power Energy Syst 2013;47:140-6.

[11] Siano P, Chen P, Chen Z, Piccolo A. Evaluating maximum wind energy exploitation in active distribution networks. IET Gener Transm Distrib 2010;4(5):598-608.

[12] Al Kaabi S S, Zeineldin H H, Khadkikar V. Planning active distribution networks considering multi-DG configurations. IEEE Trans Power Syst 2014;29(2):785-93.

[13] Hung D Q, Mithulananthan N, Lee K Y. Optimal placement of dispatchable and nondispatchable renewable DG units in distribution networks for minimizing energy loss. Int J Electr Power Energy Syst 2014;55:179-86.

[14] Tanwar S S, Khatod D K. Techno-economic and environmental approach for optimal placement and sizing of renewable DGs in distribution system. Energy 2017;127:52-67.

[15] Atwa Y M, El-Saadany E F. Optimal allocation of ESS in distribution systems with a high penetration of wind energy. IEEE Trans Power Syst 2010;25(4):1815-22.

[16] Sedghi M, Ahmadian A, Aliakbar-Golkar M. Optimal storage planning in active distribution network considering uncertainty of wind power distributed generation. IEEE Trans Power Syst 2016;31(1):304-16.

[17] Santos S F, Fitiwi D Z, Shafie-Khah M, Bizuayehu A W, C. Cabrita M P, Catalao J P S. New multistage and stochastic mathematical model for maximizing RES hosting capacity-part I: problem formulation. IEEE Trans Sustainable Energy 2017;8(1):304-19.

[18] Saboori H, Hemmati R. Maximizing DISCO profit in active distribution networks by optimal planning of energy storage systems and distributed generators. Renew Sustain Energy Rev 2017;71:365-72.

[19] Hemmati R, Saboori H, Jirdehi M A. Stochastic planning and scheduling of energy storage systems for congestion management in electric power systems including renewable energy resources. Energy 2017;133:380-7.

[20] Kandil S M, Farag H E Z, Shaaban M F, El-Sharafy M Z. A combined resource allocation framework for PEVs charging stations, renewable energy resources and distributed energy storage systems. Energy 2018;143:961-72.

[21] Li Y, Feng B, Li G, Qi J, Zhao D, Mu Y. Optimal distributed generation planning in active distribution networks considering integration of energy storage. Applied Energy 2018;210:1073-81.

[22] Sardi J, Mithulananthan N, Gallagher M, Hung D Q. Multiple community energy storage planning in distribution networks using a cost-benefit analysis. Appl Energy 2017;190:453-63.

[23] Zhang Y, Meng K, Luo F, Dong Z Y, Wong K P, Zheng Y. Optimal allocation of battery energy storage systems in distribution networks with high wind power penetration. IET Renew Power Gener 2016;10(8):1105-13.

[24] Nogueira C E C, Vidotto M L, Niedzialkoski R K, de Souza S N M, Chaves L I, Edwiges T, dos Santos D B, Werncke I. Sizing and simulation of a photovoltaic-wind energy system using batteries, applied for a small rural property located in the south of Brazil. Renew Sustainable Energy Rev 2014;29:151-7.

[25] Pilo F, Jupe S, Silvestro F, Abbey C, Baitch A, Bak-Jensen B, Carter-Brown C, Celli G, Bakari K E, Fan M T, Georgilakis P, Hearne T, Ochoa L N, Petretto G, Taylor J. Planning and optimization methods for active distribution systems. Cigre Working Group C6.19; 2014 Aug. Report No.: 591. Contract No.: ISBN: 978-2-85873-289-0.

[26] Zhao M, Chen Z, Blaabjerg F. Probabilistic capacity of a grid connected wind farm based on optimization method. Renew Energy 2006;31(13): 2171-87.

[27] Mokryani G. Active distribution networks planning with integration of demand response. Solar Energy 2015;122:1362-70.

[28] Subcommittee P. IEEE reliability test system. IEEE Trans Power Appar Syst 1979;PAS-98(6):2047-54.
[29] Xiang Y, Liu J, Liu Y. Optimal active distribution system management considering aggregated plug-in electric vehicles. Electr Power Syst Res 2016;131:105-15.
[30] Davies D L, Bouldin D W. A cluster separation measure. IEEE Trans Pattern Anal Mach Intell 1979;PAMI-1(2):224-7.
[31] Leite A P, Borges C L T, Falcao D M. Probabilistic wind farms generation model for reliability studies applied to Brazilian sites. IEEE Trans Power Syst 2006;21(4):1493-501.
[32] He X, Wang W, Jiang J, Xu L. An improved artificial bee colony algorithm and its application to multi-objective optimal power flow. Energies 2015;8(4):2412-37.
[33] Deb K, Pratap A, Agarwal S, Meyarivan T. A fast and elitist multiobjective genetic algorithm: NSGA-II. IEEE Trans Evol Comput 2002;6(2):182-97.
[34] Baran M E, Wu F F. Network reconfiguration in distribution systems for loss reduction and load balancing. IEEE Trans Power Del 1989;4(2):1401-7.
[35] Baran M E, Wu F F. Optimal capacitor placement on radial distribution systems. IEEE Trans Power Del 1989;4(1):725-34.
[36] Zou K, Agalgaonkar A P, Muttaqi K M, Perera S. Distribution system planning with incorporating DG reactive capability and system uncertainties. IEEE Trans Sustainable Energy 2012;3(1):112-23.
[37] Yingli Green Energy Holding Co., Ltd. Datasheet (INT) for the PANDA BIFACIAL 60CL, http://www.yinglisolar.com/en/products/monocrystalline/panda-bifacial-60cl/; 2018 [accessed 20 August 2018].
[38] Zeng B, Wen J, Shi J, Zhang J, Zhang Y. A multi-level approach to active distribution system planning for efficient renewable energy harvesting in a deregulated environment. Energy 2016;96:614-24.
[39] Zakeri B, Syri S. Electrical energy storage systems: A comparative life cycle cost analysis. Renew Sustainable Energy Rev 2015;42:569-96.
[40] Yao W, Zhao J, Wen F, Dong Z, Xue Y, Xu Y, Meng K. A multi-objective collaborative planning strategy for integrated power distribution and electric vehicle charging systems. IEEE Trans Power Syst 2014;29(4):1811-21.
[41] Micari S, Polimeni A, Napoli G, Andaloro L, Antonucci V. Electric vehicle charging infrastructure planning in a road network. Renew Sustainable Energy Rev 2017;80:98-108.
[42] Aalami H A, Nojavan S. Energy storage system and demand response program effects on stochastic energy procurement of large consumers considering renewable generation. IET Gener Transm Distrib 2016;10(1):107-14.
[43] Zhang Q, Li H. MOEA/D: A multiobjective evolutionary algorithm based on decomposition. IEEE Trans Evol Comput 2007;11(6):712-31.

Highlights:

- Bi-level model is proposed to plan renewable energy and energy storage coordinately
- Short-term operation and long-term planning are optimized cooperatively
- Economy, reliability, and environment issues are considered with equal attention
- High-level uncertainties and temporal correlation are addressed simultaneously
- Temporal correlation between renewable energy and load demands are investigated